DOI: 10.1002/ejic.200501022

Coordination Dependence of Magnetic Properties within a Family of Related [Fe^{II}_2] Complexes of a Triazine-Based Ligand

Manuel Quesada,[a] Paul de Hoog,[a] Patrick Gamez,*[a] Olivier Roubeau,*[b] Guillem Aromí,[c] Bruno Donnadieu,[d] Chiara Massera,[e] Martin Lutz,[f] Anthony L. Spek,[f] and Jan Reedijk[a]

Keywords: Iron(II) complexes / Magnetic properties / Spin crossover / 1,3,5-Triazine / Polydentate ligands

The coordination chemistry of the polydentate ligand 2,4,6-tris(dipyridin-2-ylamino)-1,3,5-triazine (dpyatriz) with Fe^{II} has been explored, leading through variation of the counter-ion and the solvent system to the preparation of three different dinuclear complexes: $[Fe_2(dpyatriz)_2(H_2O)_2(CH_3CN)_2](ClO_4)_4$ (**1**), $[Fe_2(dpyatriz)_2(H_2O)_2(CH_3OH)_2](BF_4)_4$ (**2**) and $[Fe_2(dpyatriz)_2Cl_2](CF_3SO_3)_2$ (**3**). The X-ray structure of these compounds has revealed that besides the difference in the noncoordinated anion, complex **1** differs from complex **2** only in the nature of the terminal ligands. Bulk magnetisation studies and Mössbauer spectroscopy have shown that such a subtle difference produces a change to the crystal field on the metal atoms, originating an important disparity of the magnetic behaviour. Thus, complex **1** experiences a partial spin crossover centred at approximately 265 K, whereas complex **2** shows two uncoupled high-spin Fe^{II} centres over most of the studied temperature range, experiencing the effect of very weak antiferromagnetic coupling and/or single-ion zero-field splitting at low temperature. By contrast, complex **3**, in which the triazine ring of dpyatriz is coordinated for the first time, displays (very uncommon) ferromagnetic coupling between both Fe^{II} ions within the molecule, leading to an $S = 4$ spin ground state. A fit of the experimental data led to a value of the coupling constant of $J = +0.23\ cm^{-1}$ (using $H = -2JS_1S_2$ as the convention for the exchange Hamiltonian) and provided an estimation of $D = 0.63\ cm^{-1}$ for the ground-state axial zero-field splitting parameter.

Introduction

The controlled design of molecule-based functional materials represents one of the research lines along which nanotechnological applications may develop. The area of coordination chemistry plays a primary role in this respect, as exemplified by the spectacular progress demonstrated in the context of molecular magnetism.[1] The search for molecular magnetic materials with specific functions is very often based on the use of ligands that will give rise to predictable chemical and physical properties. For instance, it is well known that azole-based ligands have the ability to generate the appropriate type of crystal field around Fe^{II} ions, so as to prompt the appearance of the phenomenon of spin crossover (SC) within the metal atom.[2,3] Another example is the exploitation of the potential of certain ligand systems to propagate ferromagnetic interactions between paramagnetic metals with the aim of generating high-spin molecules or magnetically ordered materials. Among such ligand frameworks are (end-on) N_3^- groups[4,5] and *m*-phenylene links (the latter usually facilitating ferromagnetism through a spin-polarisation mechanism).[6,7] Even more desirable in the preparation of versatile functional materials are systems capable of exhibiting different properties by introducing subtle changes of environment or of chemical nature.

With the aim of preparing novel coordination supramolecular architectures, some of us have recently synthesised and started to use the new multinucleating ligand 2,4,6-tris-(dipyridin-2-ylamino)-1,3,5-triazine (dpyatriz, Scheme 1)[8] in coordination chemistry reactions involving various metals. The versatility of this ligand has been demonstrated by the diversity of some of the coordination compounds obtained. Thus, the reaction with $Cu(NO_3)_2$ produces a magnetically exchanged 1D coordination polymer,[9] whereas a similar reaction involving $CuCl_2$ allows the characterisation

[a] Leiden Institute of Chemistry, Gorlaeus Laboratories, Leiden University,
P. O. Box 9502, 2300 RA Leiden, The Netherlands
Fax: +31-71-5274671
E-mail: p.gamez@chem.leidenuniv.nl
[b] Centre de Recherche Paul Pascal – CNRS UPR 8641,
115 avenue du dr. A. Schweitzer, 33600 Pessac, France
Fax: +33-556845600
E-mail: roubeau@crpp-bordeaux.cnrs.fr
[c] Departament de Química Inorgànica, Universitat de Barcelona, Diagonal 647, 08028 Barcelona, Spain
[d] Laboratoire de Chimie de Coordination CNRS – Université Paul Sabatier,
205 route de Narbonne, 31077 Toulouse Cedex 4, France
[e] Dipartimento di Chimica Generale ed Inorganica, Chimica Analitica, Chimica Fisica, Università degli Studi di Parma,
Parco Area delle Scienze 17/A, 43100 Parma, Italy
[f] Bijvoet Center for Biomolecular Research, Crystal and Structural Chemistry, Utrecht University,
Padualaan 8, 3584 CH Utrecht, The Netherlands

of the trinuclear discrete molecule $[(CuCl)_3(dpyatriz)_2][CuCl_4]Cl$.[10] The same process, using $Zn(NO_3)_2$, leads to the formation of the tetranuclear molecular species $[Zn_4(dpyatriz)_2(NO_3)_8]$.[11] In these products, the dpyatriz ligands have their three dipyridylamine (dpya) chelating units engaged in coordination. By contrast, the analogous reaction with Co^{II} conduces to the dimeric complex $[Co_2(dpyatriz)_2(NO_3)_2(CH_3OH)_2](NO_3)_2$ in which each of the multidentate ligands maintains one of their dipyridyl chelating units uncoordinated. Very recently, we have discovered that using solvothermal conditions one can prepare compounds different than those formed from the corresponding reactions under normal conditions of temperature and pressure. In this manner, coordination polymers of Cu^{II}, Zn^{II} and Cd^{II} have been crystallographically characterised.[12] Despite the variety of coordination modes and structures observed, none of the complexes described so far shows the dpyatriz ligand using the N-donor of the triazine ring for coordination to a metal atom. It is conceivable that the versatility of dpyatriz can be exploited in the search of new supramolecular architectures exhibiting novel magnetic phenomena. With this aim, we engaged in exploring the reactivity of this ligand with various sources of Fe^{II}. We report herein on the ability of dpyatriz to form dinuclear complexes of magnetically exchanged Fe^{II} ions in the form of the compounds $[Fe_2(dpyatriz)_2(H_2O)_2(CH_3CN)_2](ClO_4)_4$ (**1**), $[Fe_2(dpyatriz)_2(H_2O)_2(CH_3OH)_2](BF_4)_4$ (**2**) and $[Fe_2(dpyatriz)_2Cl_2](CF_3SO_3)_2$ (**3**), as revealed by single-crystal X-ray crystallography. The nature of the terminal ligands completing the coordination sites not occupied by dpyatriz affects either the ligand field around the metal ions or the coordination mode of the multinucleating ligand, leading thus to three related complexes with very disparate magnetic properties, ranging from spin crossover (**1**), antiferromagnetic exchange (**2**) or (very uncommon for Fe) ferromagnetic coupling (**3**). The synthesis of complexes **1**, **2** and **3** and their molecular structures are described, and the reasons for their very different magnetic behaviour discussed.

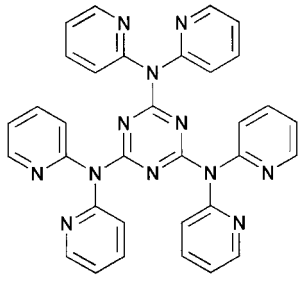

Scheme 1. Molecular structure of the ligand dpyatriz.

Results

Synthesis

In attempts to take advantage of the versatility of dpyatriz for the preparation of complexes with new and novel magnetic properties, reactions with different sources of Fe^{II} in a variety of conditions have been conducted.

Mixing in acetonitrile $Fe(ClO_4)_2$ with dpyatriz close to the 1:2 molar ratio, and small amounts of ascorbic acid (in order to avoid aerial oxidation to Fe^{III}) led to a light pink solution from which crystals could be obtained by slow diffusion of Et_2O. The identity of this compound was established by X-ray crystallography (see below) as the dimeric discrete complex $[Fe_2(dpyatriz)_2(H_2O)_2(CH_3CN)_2](ClO_4)_4$ (**1**). Water in this compound originates from the hydrated iron salt, or from its adventitious presence in the solvent. Thus, the reaction leading to the formation of **1** can be described by a very simple chemical equation [Equation (1)].

$$2\ Fe(ClO_4)_2 + 2\ dpyatriz + 2\ H_2O + 2\ CH_3CN \rightarrow [Fe_2(dpyatriz)_2(H_2O)_2(CH_3CN)_2](ClO_4)_4\ (\mathbf{1}) \quad (1)$$

It was observed that crystals of **1**, crumbled upon exposure to air and turned into a yellowish crystalline material. Elemental analysis suggested the replacement of CH_3CN molecules by H_2O, although no structural proof for the identity of the resulting material was obtained. Replacement of terminal CH_3CN ligands by atmospheric water, while maintaining the core topology, is a very common process in coordination chemistry.[13] IR spectroscopy confirmed the absence of CH_3CN in this new adduct, while the remaining spectral features were maintained.

The analogous reactivity was observed using $Fe(BF_4)_2$ and CH_3OH as a solvent. Slow evaporation of the solvent from the reaction mixture resulted in the formation of light green crystals of a new complex, the formula of which was confirmed to be $[Fe_2(dpyatriz)_2(H_2O)_2(CH_3OH)_2](BF_4)_4$ (**2**) by single-crystal X-ray diffraction (see below) and elemental analysis. Thus, Equation (1) could serve to describe the formation of **2**, only replacing CH_3CN and ClO_4^- by CH_3OH and BF_4^-, respectively. In contrast with **1**, however, this compound was found to be stable in air. The similarity of the synthesis and structure of **1** and **2** prompted us to test their interconversion. Indeed, when crystals of **1** are placed in CH_3OH, a slightly greenish powder is formed that does not turn purple when cooled to liquid N_2 temperature. Similarly, if crystals of **2** are immersed in CH_3CN, a slightly purple powder forms. Although this was not investigated further (mostly because the crystals crushed into powders), it seems that **1** and **2** can be converted into one another by simply changing their solvent environment.

Incorporation of Cl^- into a system very similar to these described above gave comparable results, although with significant differences. Thus, dpyatriz and $Fe(CF_3SO_3)_2$ were mixed in benzyl cyanide in the presence of Bu_4NCl and the solution brought to 100 °C inside a sealed pressure tube. Yellow crystals of the compound $[Fe_2(dpyatriz)_2Cl_2](CF_3SO_3)_2$ (**3**) formed under these conditions within a few days, according to the reaction described in Equation (2).

$$2\ Fe(CF_3SO_3)_2 + 2\ dpyatriz + 2\ Bu_4NCl \rightarrow [Fe_2(dpyatriz)_2Cl_2](CF_3SO_3)_2\ (\mathbf{3}) + 2\ Bu_4NCF_3SO_3 \quad (2)$$

The identity of compound **3** was unveiled by X-ray crystallography (see below), which revealed that the Cl^- ions are coordinated to Fe and that dpyatriz uses N-donors from the triazine moiety to bind the metal atom, a fact observed for the first time and bearing important consequences with regard to the magnetic behaviour of the complex. It was observed that when stoichiometric amounts of the chloride salt were used, the yields obtained were inferior compared with reactions involving limiting amounts of this reagent. A possible reason is that increased amounts of Bu_4NCl favour the formation of the dinuclear anion $[Fe_2OCl_6]^{2-}$ at the expense of complex **3**. This anion is very stable and quite ubiquitous in aerobic reactions involving Fe^{II} and chloride.[14]

Description of Structures

Crystallographic data for complexes **1**–**3** are collected in Table 4 whereas selected metric parameters are listed in Tables 1, 2 and 3.

Table 1. Selected interatomic distances [Å] and angles [°] for $[Fe_2(dpyatriz)_2(H_2O)_2(CH_3CN)_2](ClO_4)_4$ (**1**). Symmetry operation i: $1-x, 1-y, 1-z$.

Fe1–O1W	2.140(2)	N1–Fe1–N3	84.96(9)
Fe1–N1	2.160(3)	N1–Fe1–N4	100.00(9)
Fe1–N3	2.177(2)	N1–Fe1–N6	94.10(9)
Fe1–N4	2.159(2)	N1–Fe1–N13	171.01(10)
Fe1–N6	2.167(2)	N3–Fe1–N4	91.75(9)
Fe1–N13	2.151(3)	N3–Fe1–N6	175.51(9)
O1W–Fe1–N1	88.45(10)	N3–Fe1–N13	88.47(9)
O1W–Fe1–N3	90.87(10)	N4–Fe1–N6	84.08(9)
O1W–Fe1–N4	171.34(10)	N4–Fe1–N13	88.47(9)
O1W–Fe1–N6	93.50(10)	N6–Fe1–N13	89.74(10)
O1W–Fe1–N13	83.19(10)	Fe···Fe^i	9.232(2)

Table 2. Selected interatomic distances [Å] and angles [°] for $[Fe_2(dpyatriz)_2(H_2O)_2(CH_3OH)_2](BF_4)_4$ (**2**). Symmetry operation i: $1-x, 1-y, 1-z$.

Fe1–O2	2.1708(18)	O2–Fe1–N6	176.83(7)
Fe1–N1	2.167(2)	O1W–Fe1–N1	92.42(8)
Fe1–N6	2.176(2)	N1–Fe1–N4	177.02(8)
Fe1–O1W	2.0846(18)	N3–Fe1–N6	97.54(7)
Fe1–N3	2.190(2)	N3–Fe1–N4	92.02(8)
Fe1–N4	2.152(2)	N6–Fe1–N4	86.02(8)
O2–Fe1–O1W	88.07(8)	N1–Fe1–N3	87.04(8)
O2–Fe1–N3	85.57(7)	O1W–Fe1–N3	173.62(8)
O2–Fe1–N4	93.25(7)	Fe···Fe^i	9.2593(15)
O2–Fe1–N1	89.50(8)		

$[Fe_2(dpyatriz)_2(H_2O)_2(CH_3CN)_2](ClO_4)_4$ (1)

Complex **1** is a centrosymmetric cationic dimer (Figure 1) comprising two octahedral Fe^{II} ions bridged and chelated by two dpyatriz ligands through two of their dpya moieties, the third one remaining uncoordinated. The other two coordination sites on each metal atom are occupied in *cis* configuration by a molecule of H_2O and one of CH_3CN, completing an FeN_5O slightly distorted octahedral chromophore. The Fe–O and Fe–N(CH_3CN) distances are 2.140(2) and 2.151(3) Å, respectively, whereas the Fe–N(dpyatriz) distances range from 2.159(2) to 2.177(2) Å. The Fe···Fe separation is 9.232(2) Å, while the shortest intermolecular Fe···Fe distance is 8.992 Å. Four perchlorate counteranions lie between the dinuclear units and exhibit disorder of their oxygen atoms. In addition, two lattice acetonitrile molecules are found in that space. No forces other than weak electrostatic and van der Waals interactions appear to operate within the crystal. The cation of **1** is structurally analogous to the equivalent complex with Co^{II}.[11]

Table 3. Selected interatomic distances [Å] and angles [°] for $[Fe_2(dpyatriz)_2Cl_2](CF_3SO_3)_2$ (**3**). Symmetry operation ′: $-x, 1-y, 1-z$.

Fe1–Cl1	2.336(2)	N1–Fe1–N4	93.1(2)
Fe1–N1	2.229(3)	N1–Fe1–N7	76.6(1)
Fe1–N4	2.205(4)	N4–Fe1–N7	77.1(2)
Fe1–N7	2.220(4)	N1–Fe1–N11′	171.9(2)
Fe1–N11′	2.234(4)	N1–Fe1–N12′	91.8(2)
Fe1–N12′	2.215(4)	N4–Fe1–N11′	88.3(2)
Cl1–Fe1–N1	94.7(1)	N4–Fe1–N12′	168.4(2)
Cl1–Fe1–N4	97.2(1)	N7–Fe1–N11′	95.9(1)
Cl1–Fe1–N7	169.2(1)	N7–Fe1–N12′	93.9(2)
Cl1–Fe1–N11′	93.1(1)	N11–Fe1–N12′	85.5(2)
Cl1–Fe1–N12′	92.8(1)	Fe···Fe′	8.324(1)

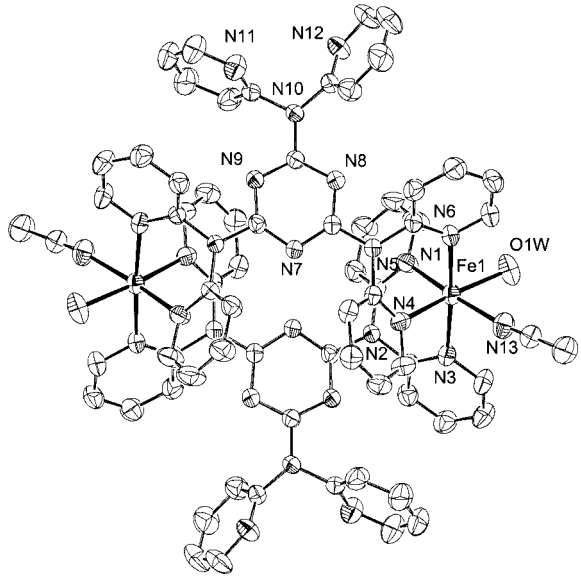

Figure 1. ORTEP representation at the 50% probability level of the cation of $[Fe_2(dpyatriz)_2(CH_3CN)_2(H_2O)_2](ClO_4)_4$ (**1**). Hydrogen atoms are not shown. Only unique non-carbon atoms are labelled.

$[Fe_2(dpyatriz)_2(H_2O)_2(CH_3OH)_2](BF_4)_4$ (2)

The structure of **2** (Figure 2) is very similar to that of **1**. It also consists of centrosymmetric Fe^{II} dinuclear entities held together by two dpyatriz ligands showing the same coordination mode. The only differences are the replacement of perchlorate by tetrafluoroborate and substitution of the CH_3CN ligand by CH_3OH. The latter difference has important consequences for the magnetic properties of the system (see below). The geometric parameters also vary slightly;

thus, the Fe–N bond lengths range from 2.152(2) to 2.190(2), whereas the Fe–O distances are 2.1708(18) Å (CH_3OH) and 2.0846(18) Å (H_2O). The intradimer Fe···Fe vector measures 9.2593(15) Å and the shortest interdimer Fe···Fe distance is 8.3577(14) Å. The BF_4^- ions are again located between the complex cations, whereas each of the two free dipyridylamine moieties accept hydrogen bonds from one CH_3OH molecule of crystallisation, thus forming a bifurcated hydrogen bond [N···O distances 3.112(3) and 2.816(3) Å].

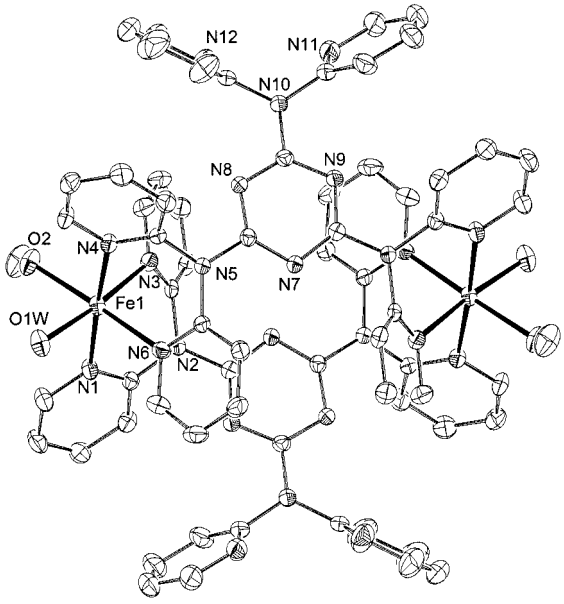

Figure 2. Labelled ORTEP representation at the 50% probability level of the cation of $[Fe_2(dpyatriz)_2(H_2O)_2(CH_3OH)_2](BF_4)_4$ (**2**). Hydrogen atoms are not shown. Only unique non-carbon atoms are labelled.

[Fe₂(dpyatriz)₂Cl₂](CF₃SO₃)₂ (3)

Also the cationic complex **3** (Figure 3) consists of a centrosymmetric dimer in which two octahedral Fe^{II} ions are connected by two dpyatriz ligands. In **3**, however, the binding mode of the multidentate ligand is very different from that observed in the two previous complexes. Here, each of the dpyatriz ligands chelates one iron cation through two nitrogen atoms from one dpya moiety and the other one with a N-donor from the triazine moiety and with two N atoms from dpya nonadjacent pyridyl rings. In this way two pyridyl rings in each dpyatriz ligand remain uncoordinated. Unlike in complexes **1** and **2**, the octahedral coordination around Fe^{II} is not completed by solvent molecules, but by a terminal Cl^- ion. The Fe1–Cl1 and Fe1–N7(triazine) distances are 2.336(2) and 2.220(4) Å respectively, while the other four Fe–N bonds involving the pyridyl groups vary from 2.205(4) to 2.234(4) Å (see Table 3). To the best of our knowledge complex **3** is the first crystallographically characterised compound where the central triazine moiety of dpyatriz is involved in coordination. The triazine rings of the two ligands lie mutually parallel although shifted with respect to each other, with a distance between the least-square planes passing through them of 3.584(1) Å. The intramolecular Fe···Fe [$-x$, $1-y$, $1-z$] separation is 8.324(1) Å, while the shortest intermolecular separation between two metal atoms is 9.041(2) Å. The two positive charges of the cationic complex $[Fe_2(dpyatriz)_2(Cl)_2]^{2+}$ are balanced by two disordered $CF_3SO_3^-$ anions located in the crystal lattice. Also two molecules of the solvent (benzyl cyanide) are present for each dimeric complex, orientated so that their CN groups point towards the triazine ring [the smallest distance of N1s to the least-squares plane passing through the ring being 3.038(9) Å].

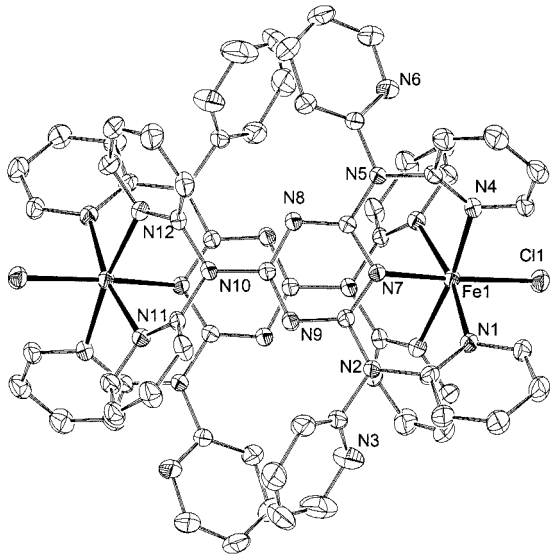

Figure 3. Labelled ORTEP representation at the 30% probability level of the cation of $[Fe_2(dpyatriz)_2Cl_2](CF_3SO_3)_2$ (**3**). Hydrogen atoms are not shown. Only unique non-carbon atoms are labelled.

Magnetochemistry

The temperature dependence of the magnetisation of compounds **1**–**3** was studied on polycrystalline samples in the 2–350 K range. This is depicted in Figures 4, 7 and 8, for **1**, **2** and **3**, respectively, in the form of $\chi_m T$ versus T plots, where χ_m is the molar paramagnetic susceptibility.

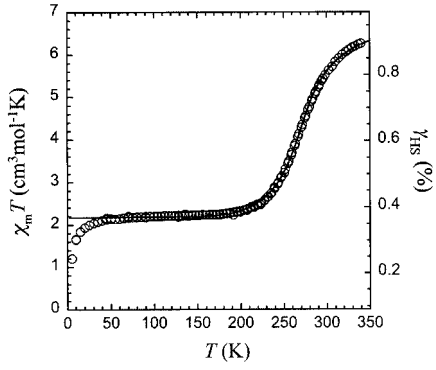

Figure 4. Plot of experimental $\chi_m T$ vs. T for compound **1** (circles) collected with an applied field of 1000 Oe. The solid line is a fit to the regular solution theory model (see text for details), expressed as the HS fraction γ_{HS}.

For compound **1** (Figure 4), the $\chi_m T$ product at 340 K is 6.27 $cm^3 \cdot mol^{-1} \cdot K$, in the range expected for two noninteracting high-spin (HS, $S = 2$) Fe^{II} centres (6 $cm^3 \cdot mol^{-1} \cdot K$, for $g = 2$). As the temperature decreases, the $\chi_m T$ value starts immediately to drop gradually to 2.2 $cm^3 \cdot mol^{-1} \cdot K$ in the vicinity of 200 K, where it remains constant upon further cooling. This is consistent with a process of SC by a fraction of the Fe^{II} centres (calculated to be 63%, see below), from HS to low spin (LS, $S = 0$). Only at very low temperatures, a decrease of $\chi_m T$ is observed anew, resulting either from zero-field splitting (ZFS) of the remaining Fe^{II} HS centres and/or from antiferromagnetic coupling of the remaining HS–HS pairs. Thus, compound **1** exhibits a gradual and incomplete SC, centred at around 265 K, but does not exhibit a plateau at $\chi_m T \approx 3.0$ (50% of Fe^{II} centres LS), which is often observed for Fe^{II} dimers undergoing a spin transition.[15,16] This indicates a lack of strong intermolecular interactions, which would stabilise domains of HS–LS pairs. In order to present a quantitative description of the process of spin transition, the Mössbauer spectra of **1** (Figure 5) were collected at 293 K (near the transition temperature) and 77 K. Signals from both the HS and LS states were detected at both temperatures. From these experiments the fraction of Fe^{II} centres in the HS state at 77 K was calculated to be 37%.[17] The temperature dependence of the HS fraction deduced from susceptibility and Mössbauer data was then fit to an equation resulting from a regular solution model [Equation (3)],[18,19] where γ_{HS} is the variable HS fraction, Γ is the interaction parameter[3] and the other terms have their usual meaning. Although it represents a crude approximation, the calculated values were normalised to the fraction of species undergoing spin crossover.

$$\ln\left(\frac{1-\gamma_{HS}}{\gamma_{HS}}\right) = \frac{\Delta H + \Gamma(1-2\gamma_{HS})}{RT} - \frac{\Delta S}{R} \quad (3)$$

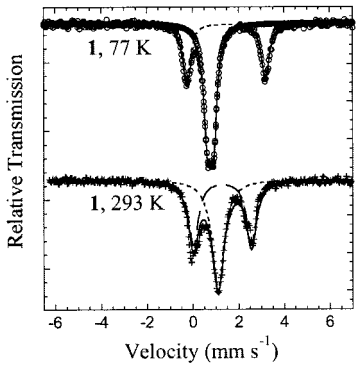

Figure 5. Mössbauer spectra of **1** at 77 and 293 K. Dashed lines represent subspectra used in the fitting procedure, while full lines are the overall fits to the experimental data.

The best fit provided (Figure 4, solid line) a value of Γ = 2.9(2) $kJ \cdot mol^{-1}$ with ΔH = 11.0(1) $kJ \cdot mol^{-1}$ and ΔS = 40(1) $J \cdot mol^{-1} \cdot K^{-1}$. The cooperativity parameter Γ is in agreement with the absence of strong interaction between the Fe^{II} centres.[3] The entropy variation deduced is about three times that expected from the change in spin manifold ($R\ln 5$ = 13.4 $J \cdot mol^{-1} \cdot K^{-1}$), indicating, as usually observed, the presence of a vibrational contribution to the entropy variation. Both the transition entropy and enthalpy derived here are in agreement with the calorimetric characterisation of weakly cooperative SC systems.[20–23] The behaviour just described is retained only if the compound is kept sealed and/or in contact with acetonitrile. If complex **1** is left exposed to air, replacement of CH_3CN by atmospheric water seems to take place (see above), the resulting material (**1a**) remaining HS throughout the whole range of temperatures.

The above results and spectroscopic evidence (see Figure 6 and below) show that the polydentate ligand dpyatriz constitutes a new member of the family of polypyridyl ligands capable of producing SC Fe^{II} compounds in the presence of the right coligands.[24–26] The system shown here is peculiar in that it is dinuclear, unlike most previously reported examples. Also, it has the potential of acting as a building block in the formation of extended structures, a very attractive prospect, as high-dimensional SC systems are still rare.

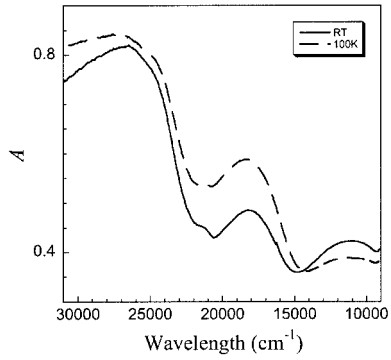

Figure 6. Absorption spectra of **1** at room temperature and about 100 K.

In contrast to complex **1**, the $\chi_m T$ product of **2** (Figure 7) remains practically constant at approximately 8.3 $cm^3 \cdot mol^{-1} \cdot K$ from room temperature to 50 K where it starts dropping to 2.65 $cm^3 \cdot mol^{-1} \cdot K$ at 2 K. This drop can

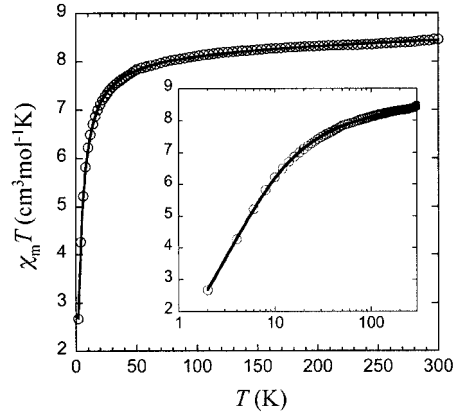

Figure 7. Plot of experimental $\chi_m T$ vs. T for compound **2**. The inset is a semi-logarithmic form of that plot. The applied field was 1000 Oe. The full line corresponds to the best fit to a theoretical expression contemplating ZFS of Fe^{II} ions (see text for details).

be ascribed either to antiferromagnetic exchange coupling within the dimeric units in **2** and/or to single-ion ZFS of the Fe^{II} centres ($S = 2$). The absence of a maximum in the χ_m versus T plot indicates that the exchange coupling is very weak. In such situations both effects, if present, are approximately of the same order and cannot be discerned. We have therefore reproduced the experimental data considering either exchange coupling [Equations (4) and (5)][18] or axial ZFS of individual Fe^{II} ions [Equations (6) and (7)],[18] including in both cases a temperature-independent paramagnetism (TIP).

$$\hat{H} = -2J(\hat{S}_1 \cdot \hat{S}_2) \quad (4)$$

$$\chi_m = \frac{N_A g^2 \beta^2}{k_B T} \cdot \frac{2e^{2x} + 10e^{6x} + 28e^{12x} + 60e^{20x}}{1 + 3e^{2x} + 5e^{6x} + 7e^{12x} + 9e^{20x}} \quad (5)$$

$$\hat{H} = 2 \times D[\hat{S}_z^2 - S(S+1)] \quad (6)$$

$$\chi_m = 2 \times \frac{N_A g^2 \beta^2}{k_B T} \cdot \left[\frac{\frac{1}{3}(2e^{-x} + 8e^{-4x}) + \frac{2}{3}\{6(1 - e^{-x})/x + 4(e^{-x} - e^{-4x})/3x\}}{1 + 2e^{-x} + 2e^{-4x}}\right] \quad (7)$$

In these expressions, D represents the single-ion ZFS parameter, J is the exchange coupling constant between Fe^{II} ions within the dinuclear entities, while x is either J/k_BT [Equation (5)] or D/k_BT [Equation (7)]. The experimental data are indeed reproduced correctly with both models, yielding on the one hand $g = 2.32(1)$, $J/k_B = -0.54(1)$ K ($J = -0.37$ cm^{-1}) and TIP = 1.6×10^{-3} $cm^3 \cdot mol^{-1} \cdot K$, and on the other hand $g = 2.41(1)$ and $D/k_B = 5.71(6)$ K ($D = 3.97$ cm^{-1}), with TIP = 1.17×10^{-3} $cm^3 \cdot K \cdot mol^{-1}$. The latter fit has a better quality (χ^2 of 0.1 compared to 0.5),[27] indicating that, although both effects are likely to be present, ZFS is probably the dominant one. The fact that the Fe^{II} centres in **2** are very weakly coupled, if at all, is consistent with the long distance mediating between them (see above) and the absence of any magnetic superexchange pathway connecting the two. On the other hand, positive values of D are often found in Fe^{II} HS species.[28]

The magnetic properties of complex **3** differ dramatically from the behaviour of the above complexes (Figure 8). The value of $\chi_m T$ at 300 K is 7.05 $cm^3 \cdot mol^{-1} \cdot K$, close to that expected for two uncoupled Fe^{II} HS centres, and remains practically constant to approximately 50 K. From that temperature, $\chi_m T$ starts to increase upon cooling to reach a maximum of 7.85 $cm^3 \cdot mol^{-1} \cdot K$ at $T = 10$ K and then suddenly drops to $\chi_m T = 4.74$ $cm^3 \cdot mol^{-1} \cdot K$ at 2 K. This behaviour is consistent with the presence of ferromagnetic exchange between the Fe centres of the dinuclear complex to form a spin ground state of $S = 4$, while the decrease of $\chi_m T$ at lower temperatures is most likely because of ZFS and not interactions between complexes, as no intermolecular exchange pathways were observed in the crystal lattice. In order to describe this behaviour quantitatively, the experimental data were fit to a $\chi_m = f(T)$ expression [Equation (8)] derived from the Van Vleck equation for two exchange Fe^{II} centres ($S = 2$), including a term D for the ZFS of the spin ground state ($S = 4$) of the dimer.[29]

$$\chi_m = \frac{N_A g^2 \beta^2}{k_B T} \cdot \frac{6e^{17x} + 24e^{8x} + 54e^{-7x} + 96e^{-28x} + 84e^{-8y} + 30e^{-14y} + 6e^{-18y}}{e^{20x} + 2e^{17x} + 2e^{8x} + 2e^{-7x} + 2e^{-28x} + 7e^{-8y} + 5e^{-14y} + 3e^{-18y}} \quad (8)$$

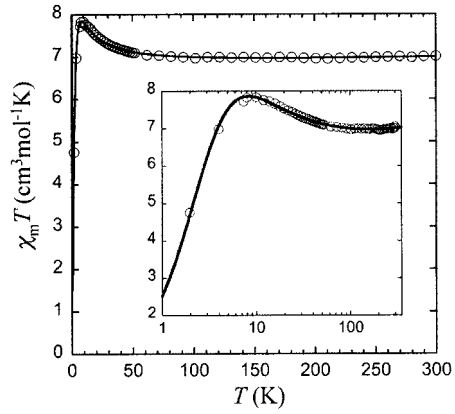

Figure 8. Plot of experimental $\chi_m T$ vs. T for compound **3**. The inset is a semi-logarithmic form of that plot. The applied field was 1000 Oe. The full lines are best fits to the corresponding theoretical expression (see text for details).

In this equation, $x = D/3k_BT$ and $y = J/k_BT$. The best fit was obtained with $g = 2.12(1)$, $J/k_B = 0.33(1)$ K ($J = 0.23$ cm^{-1}) and $D/k_B = 0.91(2)$ K ($D = 0.63$ cm^{-1}). Ferromagnetic exchange coupling between Fe^{II} centres is very uncommon.[30] A way of establishing this kind of interaction might be the mechanism of spin polarisation, by which the electronic cloud of species linking paramagnetic centres is polarised by the spin of the latter. For example, the alternation in the sign of the polarisation found within aromatic rings has allowed using them as linkers to induce predictably ferro- or antiferromagnetic interactions between spin carriers.[6] Complex **3** is the only one in the series of complexes reported here where the triazine rings are directly bound to Fe^{II} and, thus, have chances of being polarised. It is possible that the weak ferromagnetic exchange occurs through the feeble π–π interaction between these two polarised rings, despite the fact that they are shifted with respect to each other. DFT calculations will be undertaken in order to establish the nature of the magnetic orbitals participating in this superexchange and rationalise the coupling.

Solid-State Absorption Spectroscopy

Diffuse reflectance spectra of bulk **1** at 293 and about 100 K both display two very broad absorption bands centred around 11000 cm^{-1} and 18200 cm^{-1} (see Figure 6). These are typical for HS $^5T_2 \rightarrow {}^5E$ and LS $^1A_1 \rightarrow {}^1T_1$ transitions, respectively, in six-coordinate Fe^{II} showing SC. The variation in relative intensities of these bands with temperature is in agreement with the spin crossover of **1** detected by magnetic susceptibility measurements. The corresponding ligand field parameter is derived as $10Dq^{HS}$ =

11000 cm^{-1}.[31] It is known that SC behaviour is to be expected for HS species having their $10Dq^{HS}$ in the range 10500–12000 cm^{-1},[3] thus in agreement with the present observations. On the other hand, the $^5T_2 \rightarrow {}^5E$ transition in **2** is shifted towards higher energies, again in agreement with an HS ground state, and thus indicating that this compound does not show spin crossover behaviour.

Conclusions

The reactivity of the polydentate ligand 2,4,6-tris(dipyridin-2-ylamino)-1,3,5-triazine with Fe^{II} has been investigated for the first time. Small variations in reaction conditions have led to a new family of dinuclear complexes showing great diversity in magnetic behaviour. Changing solvents from CH_3CN to CH_3OH results in the change from SC behaviour in $[Fe_2(dpyatriz)_2(H_2O)_2(CH_3CN)_2](ClO_4)_4$ (**1**) to weak (or no) antiferromagnetic coupling within $[Fe_2(dpyatriz)_2(H_2O)_2(CH_3OH)_2](BF_4)_4$ (**2**). This effect is caused by the difference in crystal field produced by the solvent molecules, which in both cases act as terminal ligands. If a coordinating anion is included in the reaction, such as Cl^-, the complex $[Fe_2(dpyatriz)_2Cl_2](CF_3SO_3)_2$ (**3**) is obtained. In this case the structure of the complex differs significantly from before and Fe^{II} is seen coordinated directly to N atoms from the triazine moiety. This results in a system exhibiting very rare ferromagnetic exchange between the metal atoms. These results suggest the possibility of fine-tuning important properties of the system by choosing the type of ligand occupying the peripheral positions of the dinuclear unit, or the prospect of preparing polymeric SC systems using the appropriate dimetallic moieties as a building block.

Experimental Section

Syntheses: All reagents were used as received unless indicated otherwise. The ligand dpyatriz was prepared according to a previously published procedure.[8]

$[Fe_2(dpyatriz)_2(CH_3CN)_2(H_2O)_2](ClO_4)_4$ (1): dpyatriz (150 mg, 0.413 mmol) was added to a solution of $Fe(ClO_4)_2 \cdot 6H_2O$ (188 mg, 0.5 mmol) in acetonitrile (75 mL) and the mixture stirred. Slow diffusion of diethyl ether into this solution yielded pinkish parallelepiped crystals of $\mathbf{1} \cdot 2CH_3CN$ in 50% yield (185 mg). Complex **1** immediately lost CH_3CN upon exposure to air, presumably to be replaced by water. The resulting species may be formulated as $[Fe_2(dpyatriz)_2(H_2O)_4](ClO_4)_4$ (**1a**) (see text). $\mathbf{1a} \cdot 4H_2O$ [$C_{66}H_{64}Cl_4Fe_2N_{24}O_{24}$ (1830.86)]: calcd. C 43.30, H 3.52, N 18.36; found C 42.94, H 3.05, N 17.95.

$[Fe_2(dpyatriz)_2(H_2O)_2(CH_3OH)_2](BF_4)_4$ (2): A solution of ligand dpyatriz (200 mg, 0.34 mmol) in methanol (20 mL) was mixed, whilst stirring, with a solution of $Fe(BF_4)_2 \cdot 6H_2O$ (344 mg, 1.01 mmol) and ascorbic acid (30 mg, 0.01 mmol) in methanol (10 mL) to give a green solution. After slow evaporation of the solvent in air at room temperature (3–4 d), green crystals of $\mathbf{2} \cdot 6H_2O$ were formed in 30% yield (90 mg), which were suitable for X-ray diffraction analysis. These crystals were collected by filtration, washed with methanol and dried in air. IR: $\tilde{\nu}$ = 1001.5, 1053.9, 1373.3, 3430, 3631.1 cm^{-1}. $\mathbf{2} \cdot 6CH_3OH$ [$C_{74}H_{84}B_4F_{16}Fe_2N_{24}O_{10}$ (1928.52)]: calcd. C 46.28, H 3.99, N 17.50; found C 45.75, H 4.06, N 17.99.

$[Fe_2(dpyatriz)_2Cl_2](CF_3SO_3)_2$ (3): A solution of ligand dpyatriz (230 g, 0.387 mmol) in benzyl cyanide (99%, 25 mL) was mixed, whilst stirring, with a solution of $Fe(CF_3SO_3)_2$ (230 mg, 0.581 mmol) in benzyl cyanide (99%, 10 mL) followed by addition of ascorbic acid (30 mg, 0.01 mmol). A solution of Bu_4NCl (54 mg, 0.194 mmol) in benzyl cyanide (5 mL) was added to this mixture and the stirring maintained for several minutes. The resulting mixture was filtered and the filtrate placed into a pressure-sealed tube, which was then tightly closed and put in an oven at 100 °C. After 2 d at this temperature, yellow single crystals of $\mathbf{3} \cdot 2C_8H_7N$ suitable for X-ray diffraction were obtained. These crystals were collected and washed with methanol and diethyl ether. The yield was 15% (28 mg). IR: $\tilde{\nu}$ = 995.8, 1263.3, 1374.0 cm^{-1}. $\mathbf{3} \cdot 2C_8H_7N$ [$C_{84}H_{62}Cl_2F_6Fe_2N_{26}O_6S_2$ (1892.28)]: calcd. C 53.32, H 3.30, N 19.25; found C 53.03, H 3.54, N 19.55.

Physical Measurements: C,H,N analysis was performed with a Perkin–Elmer 2400 series. Infrared spectra (4000–300 cm^{-1} range) were recorded with a Bruker 330V IR spectrophotometer equipped with a Golden Gate Diamond. The ligand field spectra of the solids (300–2000 cm^{-1}, diffuse reflectance) were taken with a Perkin–Elmer 330 spectrophotometer equipped with a home-made set-up to measure at low temperatures (down to about 100 K). Variable-temperature and field-magnetization measurements were carried out using Quantum Design MPMS-5S and MPMS-7XL SQUID magnetometers with fields up to 5 and 7 T, respectively, and in the temperature range 2–350 K. Corrections for diamagnetic contributions to the susceptibility of the sample, as deduced from Pascal's tables, and from the sample holder were applied. Mössbauer spectra were recorded in a constant acceleration mode using a ^{57}Co in Rh source. Isomer shifts are given relative to the sodium nitroprusside. Spectra were fitted with Lorentzian-shaped lines using a non-linear iterative minimisation routine. Accuracy for the isomer shift (I.S.) is 0.03 $mm \cdot s^{-1}$, for the electric quadrupole splitting (Q.S.) 0.05 $mm \cdot s^{-1}$ and for the spectral contribution (S.C.) 5%.

X-ray Crystallographic Study: The crystal structures were determined by single-crystal X-ray diffraction methods. Crystallographic and experimental details for the different structures are summarised in Table 4. **Compound 1:** Intensity data and cell parameters were recorded at 293(2) K with a Nonius Kappa CCD diffractometer with graphite-monochromated Mo-K_α radiation (λ = 0.71073 Å). DENZO-SMN was used for data integration and SCALEPACK corrected data for Lorentz polarisation effects. Absorption corrections were applied for all data using the DIFABS program.[32] The SIR92 software package[33] and SHELXL 97, included in the WinGX package, were used for phase determination and structure refinement,respectively. Direct methods of phase determination followed by some subsequent difference Fourier maps led to an electron density map from which most of the non-hydrogen atoms were identified in the asymmetry unit of the unit cell. With subsequent isotropic refinement and Fourier difference synthesis, all of the non-hydrogen atoms were identified. Atomic coordinates, isotropic and anisotropic displacement parameters of all non-hydrogen atoms were refined by means of a full-matrix least-squares procedure on F^2. H atoms were included in the refinement in calculated positions, riding on the carbon atoms with an isotropic thermal parameter fixed 20% and 50% higher, respectively, than the sp^2- and sp^3-C atoms to which they are attached. **Compound 2:** Intensity data and cell parameters were recorded at 150 K. The structure was solved with direct methods[34] and refined with

Table 4. Crystallographic parameters of complexes **1**–**3**.

	1	**2**	**3**
Empirical formula	$[C_{70}H_{58}Fe_2N_{26}O_2](ClO_4)_4 \cdot 2C_2H_3N$	$[C_{68}H_{60}Fe_2N_{24}O_4](BF_4)_4 \cdot 6CH_3OH$	$[C_{66}H_{48}Cl_2Fe_2N_{24}](CF_3O_3S)_2 \cdot 2C_9H_7N$
Formula mass	1887.03	1928.59	1892.32
Diffractometer	Nonius KappaCCD	Nonius KappaCCD	Bruker AXS Smart 1000
Wavelength [Å]	0.71073	0.71073	0.71073
T [K]	293(2)	150(2)	293(2)
Crystal size [mm]	$0.30 \times 0.20 \times 0.05$	$0.54 \times 0.48 \times 0.12$	$0.36 \times 0.30 \times 0.24$
Crystal colour	colourless	yellow	yellow
Crystal system	triclinic	monoclinic	triclinic
Space group	$P\bar{1}$ (no. 2)	$P2_1/c$ (no. 14)	$P\bar{1}$ (no. 2)
a [Å]	11.417(2)	13.282(2)	13.250(2)
b [Å]	13.470(3)	14.499(2)	13.621(2)
c [Å]	14.100(3)	22.6080(8)	13.682(2)
α [°]	109.80(3)	90	64.419(3)
β [°]	93.60(3)	91.703(5)	70.521(3)
γ [°]	96.50(3)	90	75.965(3)
V [Å^3]	2015.2(7)	4351.8(9)	2085.6(5)
Z	1	2	1
$D_{calcd.}$ [g·cm^{-3}]	1.558	1.472	1.507
μ [mm^{-1}]	0.582	0.438	0.547
Measured reflections	12334	68949	23330
$(\sin\theta/\lambda)_{max}$ [Å^{-1}]	0.62	0.65	0.66
Abs. corr.	ψ-scans	multi-scan	multi-scan
Abs. corr. range	0.87–0.97	0.79–0.92	0.87–1.00
Unique reflections	8121	9974	9310
Parameters	649	590	547
Restraints	278	0	4
Extinction	0.0269(19)	–	–
R_1/wR_2 [$I > 2\sigma(I)$]	0.0467/0.1149	0.0506/0.1278	0.0781/0.2426
R_1/wR_2 [all refl.]	0.0604/0.1259	0.780/0.1438	0.1166/0.2726
S	1.094	1.031	0.951
$\rho_{min/max}$ [e·Å^{-3}]	–0.51/0.38	–0.63/1.10	–1.09/1.57

SHELXL-97[35] against F^2 of all reflections. All hydrogen atoms were located in the difference Fourier map. The OH hydrogen atoms were kept fixed at their located position; the other hydrogen atoms were refined as rigid groups. Drawings, geometry calculations and checking for higher symmetry were performed with the program PLATON.[36] **Compound 3:** Intensity data and cell parameters were recorded at room temperature (293 K) with a Bruker AXS Smart 1000 single-crystal diffractometer (Mo-K_α radiation) equipped with a CCD area detector. The data reductions were performed using the SAINT[37] and SADABS[38] programs. The structure was solved by direct methods using the SIR97 program[34] and refined on F_o^2 by full-matrix least-squares procedures using the SHELXL-97 program.[35] The non-hydrogen atoms were refined with anisotropic atomic displacements with the exception of the disordered triflate ion. The hydrogen atoms were included in the refinement at idealised geometries (C–H 0.95 Å) and refined "riding" on the corresponding parent atoms. The weighting scheme used in the last cycle of refinement was $w = 1/[\sigma^2(F_o^2) + (0.1687P)^2]$ (**3**), where $P = (F_o^2 + 2F_c^2)/3$. Molecular geometry calculations were carried out using the PARST97 program.[39] Drawings were obtained by ORTEP3 in the WinGX suite.[40] Calculations for **3** were carried out with a DIGITAL Alpha Station 255 computer. CCDC-224510 (**1**), -277598 (**2**) and -276288 (**3**) contain the supplementary crystallographic data for this paper. These data can be obtained free of charge from The Cambridge Crystallographic Data Centre via www.ccdc.cam.ac.uk/data_request/cif.

Acknowledgments

The authors are greatly thankful to the Dutch WFMO (Werkgroep Fundamenteel-Materialen Onderzoek), CW (Foundation for the Chemical Sciences) and NWO (Organization for the Scientific Research), to the French CNRS (Centre National de la Recherche Scientifique), to the Conseil Général d'Aquitaine, to the Spanish Ministerio de Ciencia y Tecnología for a "Ramón y Cajal" contract and to the Ministero dell'Università e delle Ricerca Scientifica e Tecnologica. R. Clérac is gratefully acknowledged for helpful discussions and M. W. J. Crajé for Mössbauer measurements.

[1] J. S. Miller, M. Drillon (Eds.), *Magnetism: Molecules to Materials V*, Wiley-VCH, Weinheim, **2005**.
[2] P. J. van Koningsbruggen in *Spin Crossover in Transition Metal Compounds I*, *Topics in Current Chemistry* (Eds.: P. Gütlich, H. A. Goodwin), **2004**, vol. 233, p. 123.
[3] P. Gütlich, A. Hauser, H. Spiering, *Angew. Chem. Int. Ed. Engl.* **1994**, *33*, 2024.
[4] A. K. Boudalis, B. Donnadieu, V. Nastopoulos, J. Modesto Clemente-Juan, A. Mari, Y. Sanakis, J.-P. Tuchagues, S. P. Perlepes, *Angew. Chem. Int. Ed.* **2004**, *43*, 2266.
[5] T. K. Karmakar, B. K. Ghosh, A. Usman, H.-K. Fun, E. Rivière, T. Mallah, G. Aromí, S. K. Chandra, *Inorg. Chem.* **2005**, *44*, 2391.
[6] F. Lloret, G. De Munno, M. Julve, J. Cano, R. Ruiz, A. Caneschi, *Angew. Chem. Int. Ed.* **1998**, *37*, 135.
[7] I. Fernandez, R. Ruiz, J. Faus, M. Julve, F. Lloret, J. Cano, X. Ottenwaelder, Y. Journaux, M. C. Muñoz, *Angew. Chem. Int. Ed.* **2001**, *40*, 3039.
[8] P. de Hoog, P. Gamez, W. L. Driessen, J. Reedijk, *Tetrahedron Lett.* **2002**, *43*, 6783.
[9] P. Gamez, P. de Hoog, O. Roubeau, M. Lutz, W. L. Driessen, A. L. Spek, J. Reedijk, *Chem. Commun.* **2002**, 1488.
[10] S. Demeshko, S. Dechert, F. Meyer, *J. Am. Chem. Soc.* **2004**, *126*, 4508.

[11] P. Gamez, P. de Hoog, M. Lutz, W. L. Driessen, A. L. Spek, J. Reedijk, *Polyhedron* **2003**, *22*, 205.
[12] H. Casellas, C. Massera, P. Gamez, A. M. Manotti Lanfredi, J. Reedijk, *Eur. J. Inorg. Chem.* **2005**, 2902–2908.
[13] G. Aromí, O. Roubeau, M. Helliwell, S. J. Teat, R. E. P. Winpenny, *Dalton Trans.* **2003**, 3436.
[14] A. Machkour, D. Mandon, M. Lachkar, R. Welter, *Inorg. Chem.* **2004**, *43*, 1545.
[15] A. B. Gaspar, V. Ksenofontov, J. A. Real, P. Gütlich, *Chem. Phys. Lett.* **2003**, *373*, 385.
[16] J. A. Real, H. Bolvin, A. Bousseksou, A. Dworkin, O. Kahn, F. Varret, J. Zarembowitch, *J. Am. Chem. Soc.* **1992**, *114*, 4650.
[17] Complex **1** (77 K) presents an HS doublet with I.S. = 1.46, Q.S. = 3.45 and relative intensity = 37%, and an LS singlet with I.S. = 0.77, Q.S. = 0.26 and relative intensity = 63%.
[18] C. J. O'Connor, *Prog. Inorg. Chem.* **1982**, *29*, 203.
[19] Note that a normalisation of the data has been performed to take into account the residual fraction of 37% at 77 K, as measured by Mössbauer spectroscopy. Such a high residual fraction, although often ascribed to defaults, may arise from a thermal equilibrium between states of the same energy ($\Delta H = 0$) but with different degeneracies and thus degrees of freedom.
[20] O. Roubeau, M. de Vos, A. F. Stassen, R. Burriel, J. G. Haasnoot, J. Reedijk, *J. Phys. Chem. Solids* **2003**, *64*, 1003.
[21] M. Sorai, Y. Maeda, H. Oshio, *J. Phys. Chem. Solids* **1990**, *51*, 941.
[22] R. Jakobi, H. Romstedt, H. Spiering, P. Gütlich, *Angew. Chem. Int. Ed. Engl.* **1992**, *31*, 178.
[23] T. Nakamoto, Z. C. Tan, M. Sorai, *Inorg. Chem.* **2001**, *40*, 3805.
[24] H. Toftlund, *Coord. Chem. Rev.* **1989**, *94*, 67.
[25] N. Moliner, M. C. Muñoz, P. J. van Koningsbruggen, J. A. Real, *Inorg. Chim. Acta* **1998**, *274*, 1.
[26] K. H. Sugiyarto, D. C. Craig, A. D. Rae, H. A. Goodwin, *Aust. J. Chem.* **1994**, *47*, 869.
[27] This value is the sum of the squared error between the original data and the calculated curve fit. In general, the lower the χ^2 value, the better the fit. The equation used to calculate χ^2 is: $\chi^2 = \sum_i (\frac{y_i - x_i}{\sigma_i})^2$, where σ_i is the weight, y_i is the actual value and x_i is the calculated value.
[28] R. L. Carlin, *Magnetochemistry*, Springer-Verlag, Berlin, **1985**.
[29] O. Kahn, *Molecular Magnetism*, VCH, New York, **1993**, p. 17.
[30] H. Oshio, N. Hoshino, T. Ito, M. Nakano, *J. Am. Chem. Soc.* **2004**, *126*, 8805.
[31] The ligand field strength $10Dq^{HS}$ can be determined directly from the ligand field spectrum, using the maximum of the $^5T_2 \rightarrow {}^5E$ transition. A good approximation to the ligand field strength of the low-spin state can be obtained from the corresponding spectrum using $10Dq^{LS} = E(^1T_1) - E(^1A_1) + [E(^1T_2) - E(^1T_1)]/4$. Unfortunately, the transition $^1A_1 \rightarrow {}^1T_2$ is not observed clearly in **1**, probably because of overlap with metal to ligand charge transfer.
[32] N. Walker, D. Stuart, *Acta Crystallogr. Sect. A* **1983**, *39*, 158.
[33] A. Altomare, G. G. Cascarano, C. Giacovazzo, A. Guagliardi, *J. Appl. Crystallogr.* **1993**, *26*, 343.
[34] A. Altomare, M. C. Burla, M. Camalli, G. L. Cascarano, C. Giacovazzo, A. Guagliardi, A. G. G. Moliterni, G. Polidori, R. Spagna, *J. Appl. Crystallogr.* **1999**, 115.
[35] G. M. Sheldrick, *SHELXL-97, Program for Crystal Structure Refinement*, University of Göttingen, **1997**.
[36] A. L. Spek, *J. Appl. Crystallogr.* **2003**, *36*, 7.
[37] *SAINT, Software Users Guide*, Bruker Analytical X-ray Systems, version 6.0, **1999**.
[38] G. M. Sheldrick, *SADABS: Area-Detector Absorption Correction*, version 2.03, University of Göttingen, **1999**.
[39] M. Nardelli, *J. Appl. Crystallogr.* **1996**, 296.
[40] L. J. Farrugia, *J. Appl. Crystallogr.* **1997**, *30*, 565.

Received: November 16, 2005
Published Online: February 6, 2006

